ORIGINAL ARTICLE

Chatter stability prediction and detection during high-speed robotic milling process based on acoustic emission technique

Maojun Li[1,2] · Dingxiao Huang[1] · Xujing Yang[1]

Abstract

Chatter as a common and thorny problem occurs easily during robotic milling process, leading to the instability, severe tool wear and poor surface finish. In this work, an acoustic emission technique was employed to analyze a chatter phenomenon using root mean square (RMS) value and fast Fourier transform method during high-speed robotic milling of aluminum alloys (with cutting speed up to 678 m/min). A stability lobe diagram was proposed to predict the occurrence of chatter with various spindle speeds, which was considered as the most effective tool for chatter analysis. The underline mechanism and theoretical analysis were also presented to provide physical understanding of chatter stability. The cutting force model and robot structure model were firstly established to study chatter mechanism. The stability of a robotic milling system was then analyzed using a zero-order approximation method. Results showed that fast Fourier transform and the time-domain root mean square (RMS) value of acoustic emission signals could be effectively used for detection and verification of chatter in the robotic milling process. The stable cutting zone in the stability lobe diagram was in agreement with experimental results, which can help for the selection of reasonable cutting parameters to avoid chatter and improve efficiency during the high-speed robotic milling process.

Keywords Chatter stability · Acoustic emission · Robotic milling · Stability lobe diagram

1 Introduction

Compared with a computer numerical controlled (CNC) machining center, applying industry robot for machining presents many advantages including good processing space accessibility, flexible tool shaft control, high space utilization and good economic performance. However, problems such as low rigid, poor positioning accuracy and repeated positioning accuracy are limiting the development of industry robot. Vibration/chatter during the cutting process is the common phenomenon due to the low rigid of robots. The stiffness of articulated robots is usually less than 1.0 N/μm, while the stiffness of standard CNC machine tools is often greater than 50.0 N/μm [1]. Low rigidity resulting in chatter becomes a common phenomenon in the robotic milling process. Moreover,

chatter has many hazards, such as deteriorating machined surface, limiting the efficiency of machining, generating noise pollution, reducing the tool life span or even damaging the machine spindle bearing [2]. Therefore, in order to improve the production efficiency using industrial robots and reduce costs, it is necessary to analyze the stability of industrial robots [3].

Industrial robot milling vibration includes free vibration, forced vibration and self-excited vibration. When the source of vibration is detected, free vibration and forced vibration can be eliminated, or even avoided [4]. However, self-excited vibration is generated inside the system, the mechanism is more complicated and it is difficult to directly avoid or eliminate. Yue et al. [5] found that the main sources of self-excited vibration during the milling process were modal coupling chatter and regenerative chatter. When the stiffness difference was small, the system was prone to generate modal coupling chatter [6]. Moreover, when the rigidity of the structure was not significantly higher than the machining rigidity, or the axis with less rigidity was within the angle formed by the total cutting force and the normal direction of the workpiece surface, the modal coupling chatter was likely to occur [7]. Tunc and Stoddart [8] found that based on the change of the robot's

✉ Maojun Li
  maojunli@hnu.edu.cn

1   State Key Laboratory of Advanced Design and Manufacture for
    Vehicle Body, Hunan University, Changsha 410082, Hunan, China

2   State Key Laboratory of High Performance Complex Manufacturing,
    Central South University, Changsha 410083, Hunan, China

posture, the occurrence of chatter could be avoided by changing the robot's feed direction and path. Gasparetto [6, 9] and Verl et al. [10] found that there were two important influencing factors of modal coupling chatter, one was the angle r between the direction of average resultant force and the direction of the maximum main stiffness of industrial robot, and the other was the difference between the two main stiffness directions. The reduction of angle r could suppress modal coupling chatter. However, this might change the feed direction of the system and the positioning of workpiece, which limited the flexibility and versatility of the milling process. Cen and Shreyes [11] proposed a new method using conservative congruence transformation (CCT) stiffness model to avoid mode coupling chatter in the robot milling process, which did not need to change the tool feed or workpiece direction and was more effective in the weak stiffness work zone, where model coupling chatter was more likely to occur. The most significant cause of regenerative chatter was the variation of cutting thickness [12]. When the fluctuation of cutting thickness reached the conditions required for self-excited vibration, the system would generate regenerative chatter. Gasparetto [6] found that regenerative chatter in the CNC machining center usually preceded modal coupling chatter, which was rarely concerned. However, due to the low stiffness and coupling structure of industrial robot, both regenerative chatter and modal coupling chatter should be considered [13].

Currently, the widely used stability prediction method is to draw the system lobe diagram [14]. In order to draw the stability lobe diagram, the milling system model should be firstly developed, and then appropriate stability analysis methods are used to characterize system stability, such as zero-order approximation, semi-discrete and full-discrete. In order to analyze the stability of the milling system, Altintas and Budak [15] proposed a zero-order approximation method by frequency model using Fourier series expansion of the direction coefficients, which ignores the influence of higher harmonics and only retains the zero-order, and a semi-discretization method by time model is presented by Insperge and Stépán [16]. Ding et al. [17] proposed a full-discrete method discretizing the state term and delay term by linear interpolation.

The parameters of the stability lobe diagram include the modal parameters and cutting force coefficient. The modal parameters mainly include modal stiffness, natural frequency and damping ratio. The acquisition of modal parameters should firstly obtain the frequency response function of industrial robot through a hammering experimenter or a Doppler analyzer, then use appropriate fitting and identification methods to obtain each order of modalities. David et al. [18] found that the cross term of frequency response function matrix affected the system dynamics. If the asymmetry was not considered, it would lead to inaccuracy of the stability lobe diagram. Cordes et al. [13] found that in the high-speed

milling process, the system stability is mainly determined by 5, 6, 7 and 8 modes, and the type of chatter is mainly regenerative chatter.

In recent years, a variety of sensors and corresponding signals have been used to detect chatter including cutting force [19, 20], acceleration [21] and sound [22]. Comparing with the performance of other sensors, acoustic emission (AE) detection has many advantages including without affecting the cutting process or damaging the instrument, high sensitivity and wide frequency range. As acoustic emission is defined as a physical phenomenon in which instantaneous elastic waves are generated within the material due to the rapid release of energy, the vibration can produce acoustic emission signals [23]. They were employed to monitor the machining process, while limited research information can be found about the correlations between high-speed robotic milling chatter and characteristics of acoustic emission signals. The chatter frequency and change of time-domain amplitude are important values of acceleration sensor and force sensor to characterize chatter phenomenon. However, the signal sources of the AE sensor during the machining process mainly include tool fracture and the friction between tool and workpiece. Moreover, industrial robot presented relatively low natural frequency due to its low stiffness, and the stiffness of robot varied with different pose [24, 25]. Therefore, it is difficult to detect chatter only by chatter frequency and the change of time-domain amplitude for acoustic emission signals.

In this work, the chatter stability of robotic milling is detected and predicted. The RMS values, maximum amplitude and non-dominant frequency amplitude after 2500-Hz low-pass filtered are used as characteristic values to characterize chatter phenomenon and the system stability is predicted using zero-order approximation with X, Y and Z directions.

2 Robotic milling dynamics modeling

The dynamic modeling of the robotic milling system is shown in Fig. 1. The dynamic equations considering the X, Y and Z directions for the tool-workpiece system can be obtained as

$$M \begin{bmatrix} \ddot{x}(t) \\ \ddot{y}(t) \\ \ddot{z}(t) \end{bmatrix} + C \begin{bmatrix} \dot{x}(t)\,\dot{y}(t)\,\dot{z}(t) \end{bmatrix} + K \begin{bmatrix} x(t) \\ y(t) \\ z(t) \end{bmatrix} = \begin{bmatrix} F_x(t) \\ F_y(t) \\ F_z(t) \end{bmatrix} \quad (1)$$

where $M = \begin{bmatrix} m_{xx} & m_{xy} & m_{xz} \\ m_{yx} & m_{yy} & m_{yz} \\ m_{zx} & m_{zy} & m_{zz} \end{bmatrix}$, $C = \begin{bmatrix} c_{xx} & c_{xy} & c_{xz} \\ c_{yx} & c_{yy} & c_{yz} \\ c_{zx} & c_{zy} & c_{zz} \end{bmatrix}$

and $K = \begin{bmatrix} k_{xx} & k_{xy} & k_{xz} \\ k_{yx} & k_{yy} & k_{yz} \\ k_{zx} & k_{zy} & k_{zz} \end{bmatrix}$ are the mass matrix, damping matrix and stiffness matrix, respectively. $F_x(t)$, $F_y(t)$ and $F_z(t)$ indicate the component forces in the X-axis, Y-axis
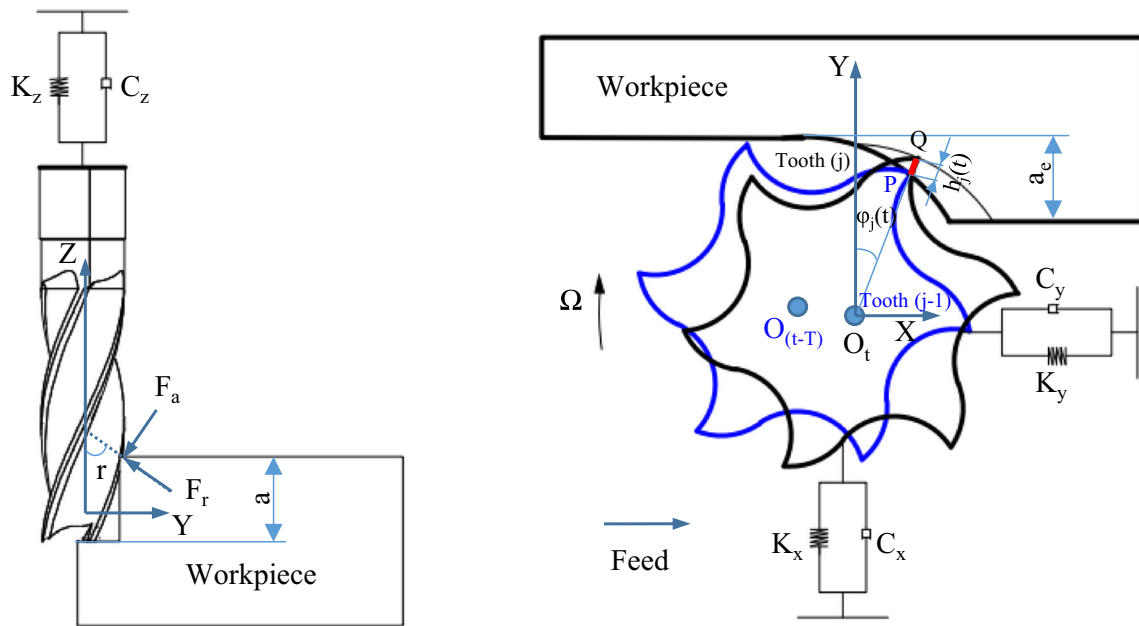
Fig. 1 The dynamic modeling of the milling system in X, Y and Z directions

and Z-axis directions, and x(t), y(t) and z(t) represent the displacement of cutting tool in the X, Y and Z directions. Generally, in the robotic milling process, the system matrices are dependent on the posture of robot. Therefore, in order to reduce the stiffness change of the robot milling system, the milling trials were conducted with the same path and starting point.

2.1 Milling force model

The robot chatter mainly includes regenerative chatter and modal coupled chatter, and periodic changes in cutting force and cutting thickness are important characteristics of chatter. Therefore, it is assumed that the tangential $F_{t,j}$, normal $F_{r,j}$ and axial $F_{a,j}$ at the jth tooth are proportional to the axial depth of cut a_p and chip $h_j(t)$:

$$\begin{bmatrix} F_{t,j} \\ F_{r,j} \\ F_{a,j} \end{bmatrix} = a \left\{ \begin{bmatrix} K_t \\ K_r \\ K_a \end{bmatrix} h_j(t) + \begin{bmatrix} K_{te} \\ K_{re} \\ K_{ae} \end{bmatrix} \right\} \quad (2)$$

where a is axial depth of cut, K_t, K_r and K_a are tangential, normal and axial linearized cutting force coefficients respectively, and K_{te}, K_{re} and K_{ae} are the edge cutting force coefficient which can be ignored during stability analysis. As shown in the Fig. 1, at time t, the instantaneous cutting thickness $h_j(t)$ depends on the current position Q of tooth (j) and the position P of tooth ($j-1$) at time ($t-T$). It is assumed that the stiffness of robot is constant in a short time interval, and the cutting thickness can be approximated as

$$h_j(t) = g\big(\varphi_j(t)\big) \begin{bmatrix} \sin\varphi_j(t)\sin r \\ \cos\varphi_j(t)\sin r \\ -\cos r \end{bmatrix}^T \begin{bmatrix} x(t)-x(t-T) \\ y(t)-y(t-T) \\ z(t)-z(t-T) \end{bmatrix} \quad (3)$$

where the tooth passing period $T = 60/\Omega N$ represents the rotation period of a single tooth at a spindle speed of Ω (rev/min), r is the axial immersion measured from the tool tip in the spindle (Z) axis and the function $g(\varphi_j(t))$ is defined as

$$g\big(\varphi_j(t)\big) = \begin{cases} 1 & \text{if } \varphi_{st}(t) < \varphi_j(t) < \varphi_{ex}(t) \\ 0 & \text{otherwise} \end{cases} \quad (4)$$

where φ_{st} and φ_{ex} are the cut-in and the cut-out angle of tooth j, the radial immersion angle $\varphi_j(t) = (2\pi\Omega/60t + 2\pi(j-1)/N)$ is the instantaneous angular immersion of tooth (j) measured clockwise from the normal (Y) axis and N is the cutting edges. According to coordinate transformation and force superposition, the X, Y and Z cutting forces acting on the tool can be expressed as

$$\begin{bmatrix} F_x \\ F_y \\ F_z \end{bmatrix} = \sum_{j=1}^{N} \left\{ \begin{bmatrix} -\cos\varphi_j(t) & -\sin\varphi_j(t)\sin r & -\sin\varphi_j(t)\cos r \\ \sin\varphi_j(t) & -\cos\varphi_j(t)\sin r & -\cos r\cos\varphi_j(t) \\ 0 & \cos r & -\sin r \end{bmatrix} \begin{bmatrix} F_{t,j} \\ F_{r,j} \\ F_{a,j} \end{bmatrix} \right\} \quad (5)$$

2.2 Stability prediction analysis

According to the robotic milling dynamics modeling and the zero-order approximation method presented by Altintas, the stability of the robotic milling system can be solved in

frequency [15]. The stability of the system is determined by the characteristic equation as

$$\det[[I] + \Lambda[G_0(iw_c)]] = 0 \tag{6}$$

where w_c is the chatter frequency, Λ is the characteristic value and $G_0(iw_c)$ represents the direction transfer function. Since the axial depth of cut a_{lim} is a real number, the critical axial milling depth and spindle speed can be obtained as

$$a_{lim} = -\frac{2\pi\Lambda_R}{NK_t}\left(1 + \frac{\Lambda_I{}^2}{\Lambda_R{}^2}\right) \tag{7}$$

$$\Omega = \frac{60w_c}{N((2k+1)\pi - 2\tan^{-1}(\Lambda_I/\Lambda_R))} \tag{8}$$

where Λ_R and Λ_I refer to the real and imaginary parts of characteristic value, and k is the frame of cutting vibration ripple.

3 Robotic milling trials with acoustic emission technique

3.1 Setup for robotic milling trials

In order to detect the chatter phenomenon using the acoustic emission technique, milling trials were conducted on the industrial robot machining system, as shown in Fig. 2. The six-axis industrial robot applied for the experiment was supplied by KUKA (KR210R2700), which was integrated with KRC4 control system and a heavy spindle HSD Mechatronic ES929 delivering spindle speeds up to 20,000 rpm. The robot was programmed via CAD/CAM Robot-master software and could handle a payload of 210 kg. The positioning accuracy and pose repeatability (ISO 9283) of the industrial robot were ± 0.7 mm (full stroke) and ± 0.06 mm, respectively. Aluminum alloy 6061 was selected as the workpiece materials, which was the alloy of aluminum with magnesium and silicon as two main elements, providing the minimum tensile and yield strength of 300 and 240 MPa, respectively. It was widely used in aerospace and advanced automotive industries. The specimen with the dimensions of 400 mm × 70 mm × 5 mm was mounted on the machining table rigidly using vice fixture. Cutting tools employed for this work were 12.0-mm-diameter tungsten carbide 6-flute end mills (supplied by NTS Cutting Tools Co., Ltd.). For all the experimental trials, the spindle speed varied from 4000 to 18,000 rpm, and the axial and radial depth of cut were kept constant at 5 mm and 0.2 mm, respectively. Down milling under dry cutting conditions was performed for all trials, with the posture of industrial robot shown in Fig. 3. The detailed experimental trials with corresponding operating parameters are presented in Table 1. The acoustic emission sensor was located close to workpiece materials with sampling rate of 2 MHz, and PCI-2 data

acquisition card was used to recorded acoustic emission signals for chatter and stability analysis. In order to ensure that the sensor was closely attached to the surface of workpiece and reduce the attenuation of AE signal transmission, a vaseline acoustic coupling agent was applied to the surface of sensor and workpiece.

## 3.2 Mechanisms of using acoustic emission to detect robotic milling chatter

In Fig. 4, the AE detection system included AE R6α sensor, 2/4/6 preamplifier and AE win^{TM} software in the robotic milling process. It is well known that acoustic emission is defined as a physical phenomenon in which instantaneous elastic waves are generated within the material due to the rapid release of energy [26]. In the cutting process, the major sources for AE waves include the shear deformation of workpiece in the first deformation zone (shear zone), the plastic deformation of workpiece and the sliding friction between tool and chip in the second deformation zone (chip-tool interface), extrusion and friction between flank face and newly formed surface of workpiece in the third deformation zone (tool flank-workpiece interface), the plastic deformation and breakage in the chip, collisions between chip and tool, tool vibration, and chipping and fracture of the tool [26–28], as the details shown in Fig. 5. Moreover, according to the reference [2], the occurrence of robotic milling chatter causes periodic changes in cutting force, noise generation and deterioration of the surface quality. Therefore, the AE sensor can be used for effectively detecting robotic milling chatter.

4 Analysis of acoustic emission signals during robotic milling

4.1 Time-domain analysis of acoustic emission signals

The AE signals were obtained based on the AE measuring system during the process of robotic milling. The duration of tool-workpiece contact was too short that the traditional methods of AE signal processing, like burst counting, could not be applied [29]. As the AE signal is sensitive to response, the change of energy wave and different cutting condition showed different AE energy characteristics in the milling process; this work used the sudden variation of AE energy to characterize system stability. In Fig. 6, it was found that the milling cut-in and cut-out stages had a huge effect on the time-domain signals. To improve the detection accuracy of AE signals, for all of the experimental trials, time spacing was employed, which was intercepted by a suitable rectangular [30]. The RMS characteristics of time-domain acoustic emission signal with the same time interval (0.1 s) are shown in Fig. 7. It was noted that as the spindle speed increased, the

Fig. 2 Experimental setup of the robotic milling process with the AE system
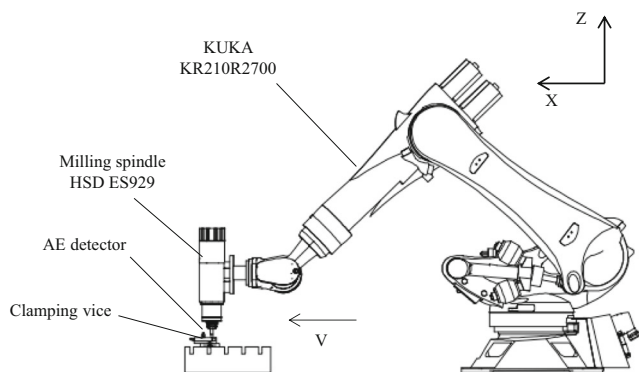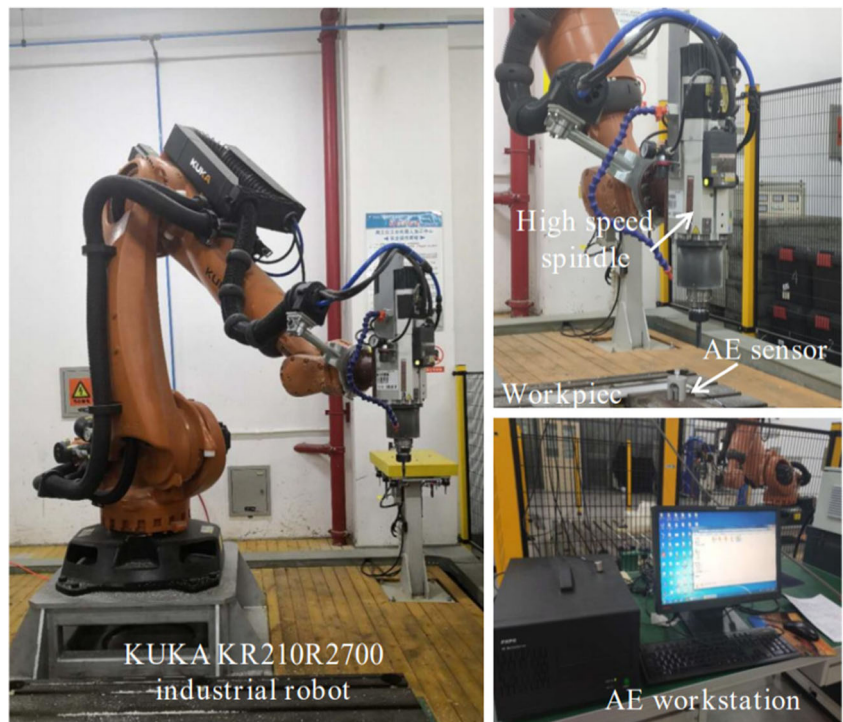
Fig. 3 Schematic picture showing robot posture during the down milling process

RMS value showed an increasing trend. This phenomenon was consistent with the results obtained by previous research, which indicated that the higher RMS of an AE signal correlated with a higher spindle speed [31]. However, the RMS values of groups A6 and A7 were 0.672 V and 0.688 V respectively, which reduced by ~15% compared with results from group A5, and the RMS value of group A10 was only 81% of corresponding value from group A9. Since the sudden change of the RMS value was mainly caused by the change of the cutting condition, the stability should be presented in groups A6, A7 and A10.

4.2 Frequency domain analysis of acoustic emission signals

Although the occurrence of stability could be observed from the time-domain analysis of AE signals according to the

Table 1 Test matrix of experimental trials with detailed operating parameters

Test group	Axial depth of cut (mm)	Spindle speed (rpm)	Test group	Axial depth of cut (mm)	Spindle speed (rpm)
A1	5.0	4000	A7	5.0	10,000
A2	5.0	5000	A8	5.0	11,000
A3	5.0	6000	A9	5.0	12,000
A4	5.0	7000	A10	5.0	14,000
A5	5.0	8000	A11	5.0	16,000
A6	5.0	9000	A12	5.0	18,000
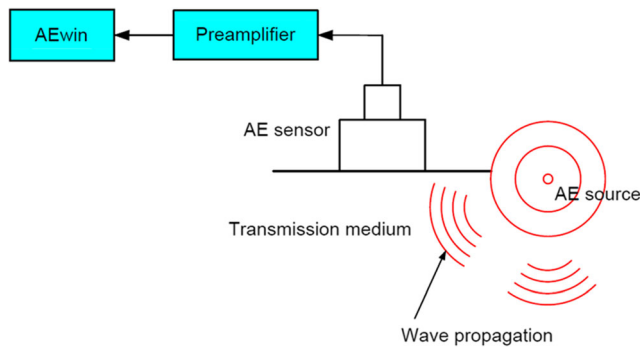
Fig. 4 Schematic diagram showing acoustic emission detection system

Fig. 7 The variations of RMS values of acoustic emission signals with different spindle speeds

mutation of RMS, it was difficult to distinguish the experimental group whose RMS value did not change significantly due to the influence of different spindle speed. Fig. 8a indicates that it is difficult to distinguish the cutting condition of the robotic milling process through AE time-domain signals, which are different from acceleration and cutting force sensor. It is well known that chatter frequency is the most direct feature to characterize chatter processing in different chatter states (slight chatter, severe chatter), which is mainly located

near the natural frequency, and the tooth passing frequency, spindle rotation frequency as well as chatter frequency are important characteristic values representing vibration [32]. Therefore, in order to effectively pay attention to the change

Fig. 5 Schematic diagram showing the main sources of acoustic emission during the metal cutting process
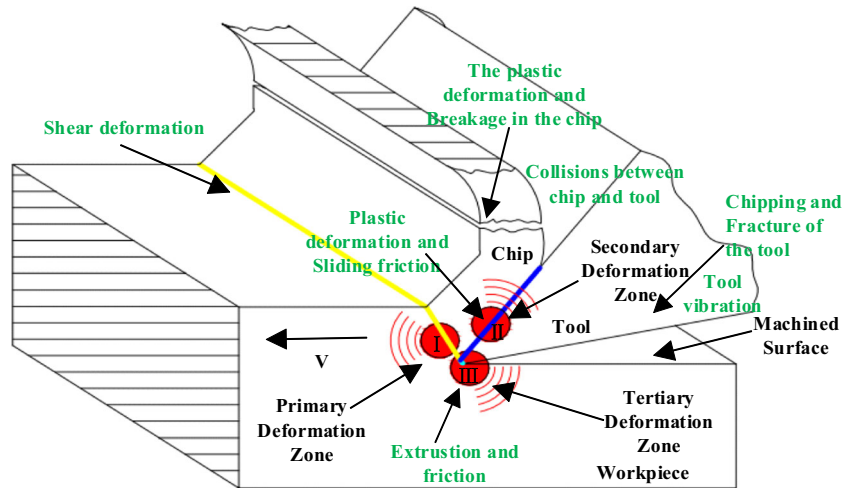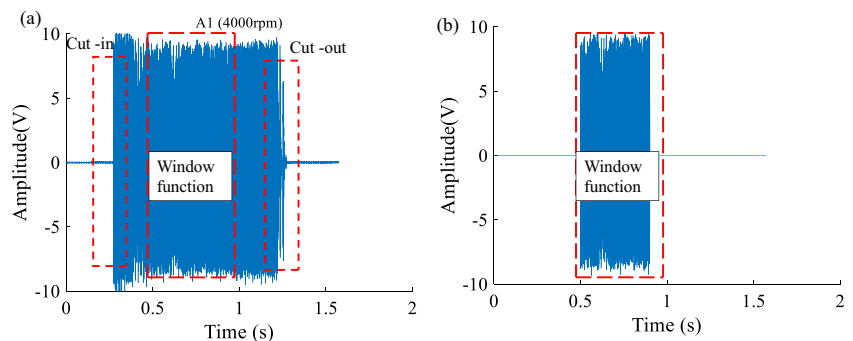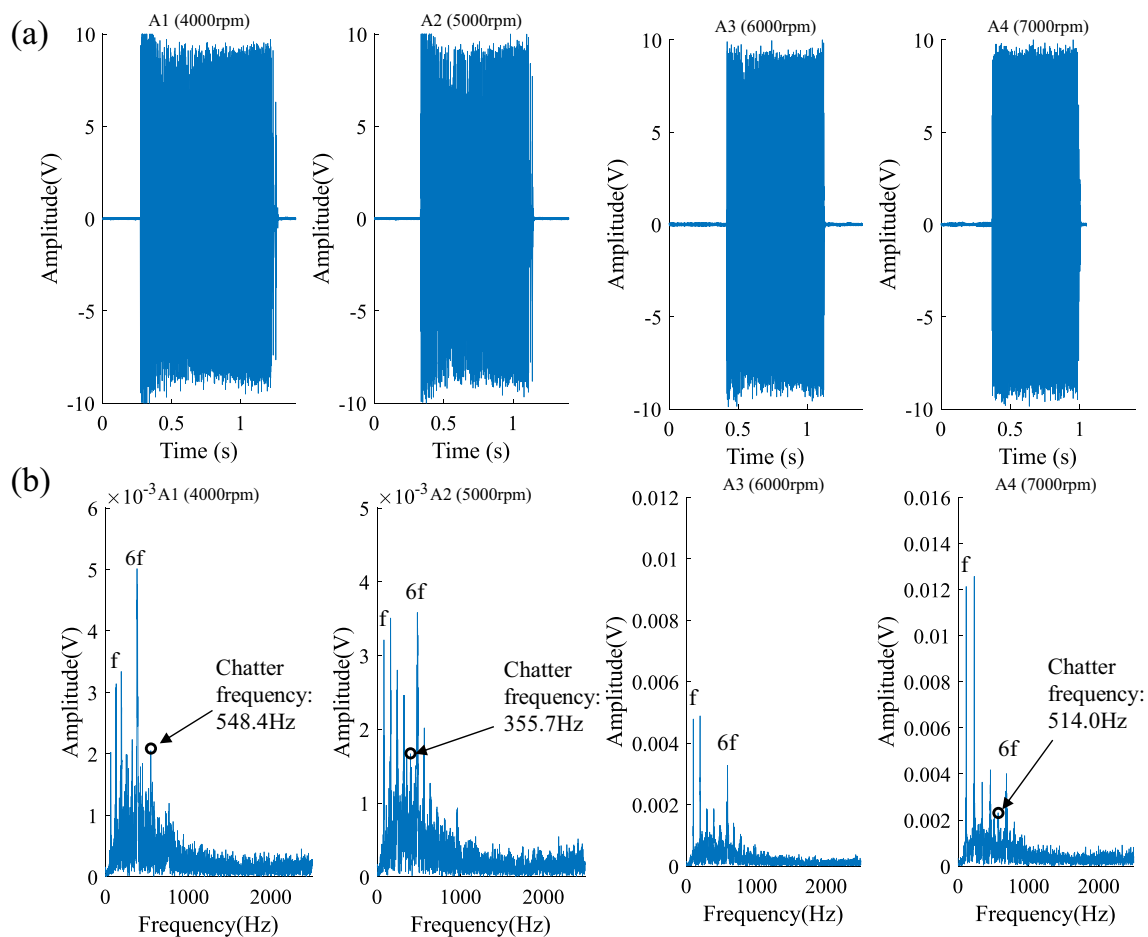

Fig. 6 The pre-processing of time-domain acoustic emission signals from the robotic milling trial with spindle speed of 4000 rpm

Fig. 8 The time-domain (a) and frequency-domain (b) AE signals for groups A1 to A4

of characteristic frequency, the AE signals were analyzed using fast Fourier transform (FFT) by MATLAB software. The representative AE signals in the frequency domain by 2500 Hz low-pass filtered are illustrated in Fig. 8b. f denoted their spindle speed frequency, and 6f denoted their tooth passing frequency. In the robotic milling process, the dominant frequency in the AE frequency domain was mainly composed of the chatter frequency, the spindle speed frequency and its multiplier, which were consistent with the frequency domain composition of the cutting force signals in the milling chatter detection [33]. It was clearly seen that the chatter frequency was 548.4 Hz in group A1, which was different from results in group A2 (355.7 Hz) and A4 (514.0 Hz). Since the vibration during the milling process included forced vibration and self-excited vibration, it was deduced that if the frequency components of AE signal only existed at multiples of spindle speed frequency, the vibration could be regarded as forced vibration; otherwise, it was regarded as self-excited vibration. Therefore, a chatter phenomenon appeared in groups A1, A2 and A4, and the chatter frequency was influenced by cutting speed and robotic posture. In Fig. 8b, it was noted that as the speed

increased, the amplitude of the spindle speed frequency was gradually higher than the one of tooth passing frequency. A possible explanation of this phenomenon was that the dominant frequency should be equal to the tooth passing frequency in the case of absence of tool runout, or rotation frequency if the runout was significant [29].

The chatter frequencies of robot were comparably low, and it was quite possible that the chatter frequency was located near the tooth passing frequency with low spindle speed and spindle speed frequency with high spindle speeds. This indicated that in the robotic milling process, it was difficult to detect chatter phenomena using only the chatter frequency. In order to characterize stability of robotic milling of Al alloys using the acoustic emission technique, the representative frequency-domain AE signals are shown in Fig. 9. It was noted that the maximum amplitude and amplitude of non-dominant frequency in groups A5, A8, A9, A11 and A12 (largest amplitude>0.0160V) were higher than the ones from groups A6, A7 and A10 (largest amplitude <0.0130V). Cutting with chatter vibration provided high-amplitude AE signals and noise affecting the amplitude of the non-
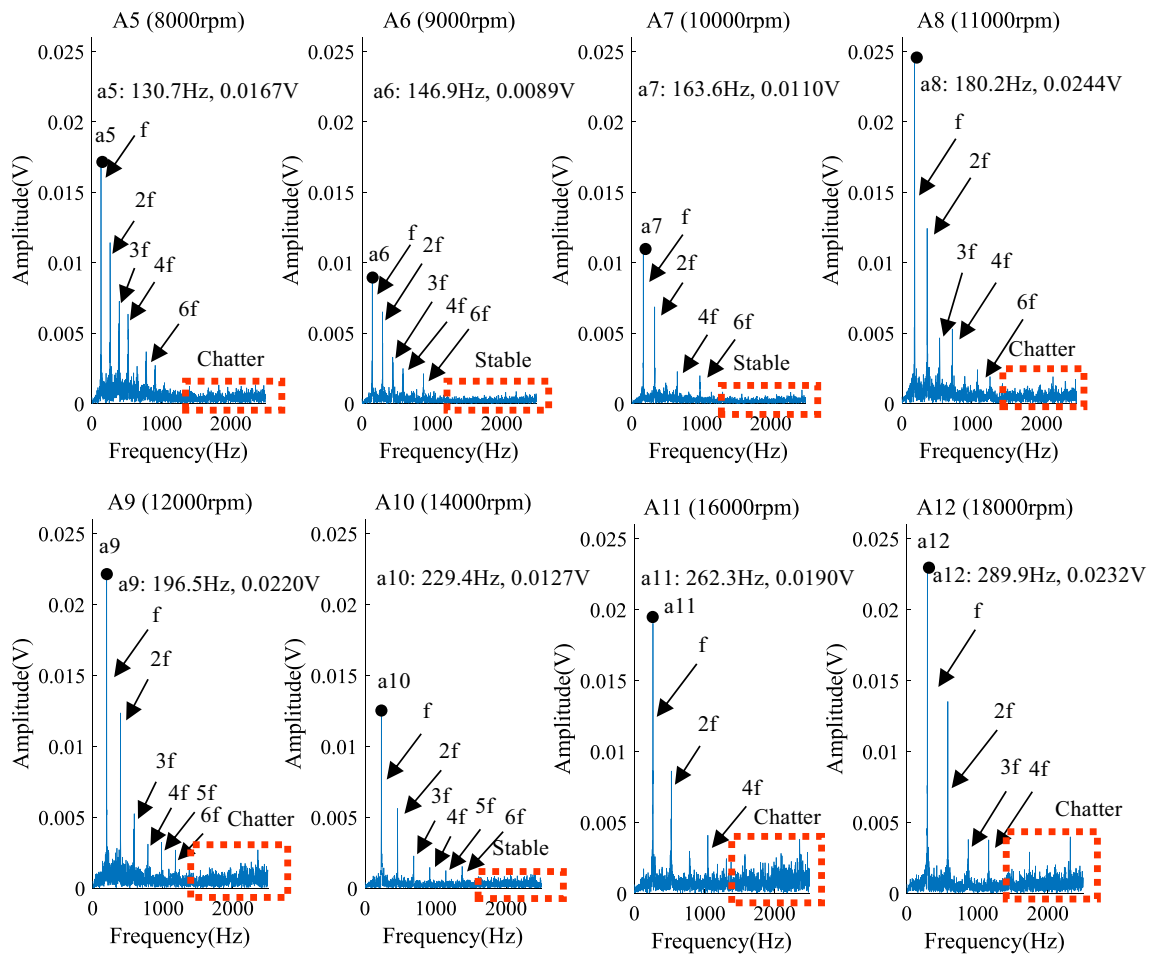
Fig. 9 Spectrum analysis of acoustic emission signals

dominant frequency [27]. Therefore, it was speculated that the stable condition/machining should occur in groups A6, A7 and A10.

5 Experimental validation

The robotic modal mass, damping and stiffness were measured by a 3D laser vibrometer (3DLVS-F), and the cutting force coefficient was obtained by identification method of the cutting force coefficient presented by Altintaş and Budak [15]. The fitted frequency response results of the first eight dominant structural modes are shown in Fig. 10. It was found that the frequency response results considering different structure modes presented different amplitudes and frequency. The frequency response results considering different structure modes were mainly concentrated in the X and Y directions (Hxx, Hyy). Moreover, there was modal cross coupling in the X, Y and Z directions (Hxy, Hyx, Hxz, Hzx, Hyz, Hzy), which affected the stability lobe diagram. It was interesting to find

that the low-order modes (1, 2, 3, 4) of robot structure were all at low frequencies (<50 Hz), but the natural frequency of high-order modes (5, 6, 7, 8) was between 500 and 2500 Hz.

Subsequently, the characteristic value (Λ_R and Λ_I) of the robot dynamics characteristic equation in the frequency domain (Eq. 11) can be calculated. The characteristic value (Λ_R and Λ_I) and the chatter frequency (w_c) around a domain mode were substituted into Eqs. 11, 17 and 19 to obtain the critical axial depth of cut and spindle speed. Finally, according to the obtained critical depth of cut and spindle speed, the stability lobe diagram can be drawn, as shown in Fig. 11. It is well known that different modes generated different stability diagrams [13]. According to the stability diagram, it was found that the stability of robotic milling Al alloy was mainly affected by the 5th and 6th modes, and the chatter occurred in groups A1 to A5, A11 and A12. The disagreement between prediction and experiment occurred in groups A8 and A9, which could be possibly due to the slight change of robotic pose during the milling process, the inevitable errors in fitting modal and cutting force coefficient and the linear approximations
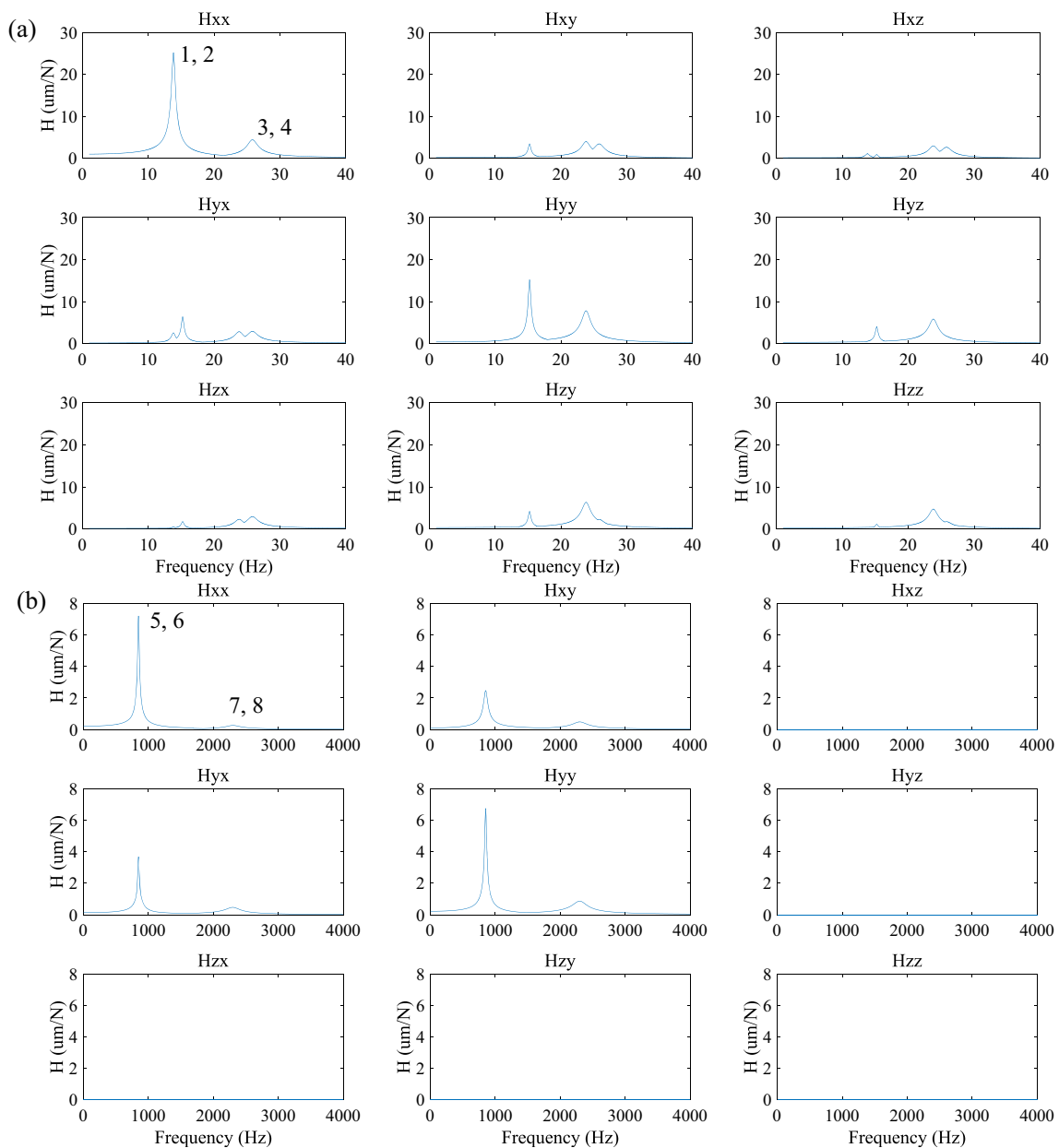
Fig. 10 The frequency response results considering (**a**) 1st, 2nd, 3rd, 4th and (**b**) 5th, 6th, 7th, 8th domain structural modes

made in the analytical solution of chatter stability. Representative finished surfaces recorded from groups A9 and A12 are shown in Fig. 12. When the chattering occurred, obvious vibration marks can be observed on the surface of the workpiece.

6 Conclusions

This paper presented an effective method for detecting robotic milling chatter based on the acoustic emission technique. The root mean square (RMS), fast Fourier transform and low-pass filtering were used to process the acoustic emission signal in the robotic milling process, which can be then applied for characterizing the stability of the robotic milling system. Since the chatter frequency was influenced by cutting speed and robotic posture, it was difficult to characterize all chatter phenomena by the chatter frequency. It was interesting to note that since the occurrence of robotic milling chatter led to the variation of energy waves, surface quality and amplitude of AE signals, when the milling state was transformed from chatter to stable, the time-domain RMS values, maximum

Fig. 11 Stability lobe diagram of robotic milling Al alloy considering the first eight dominant structural modes. Milling force coefficient: $K_t =$ 691N/mm^2, $K_r = 263$N/mm^2.
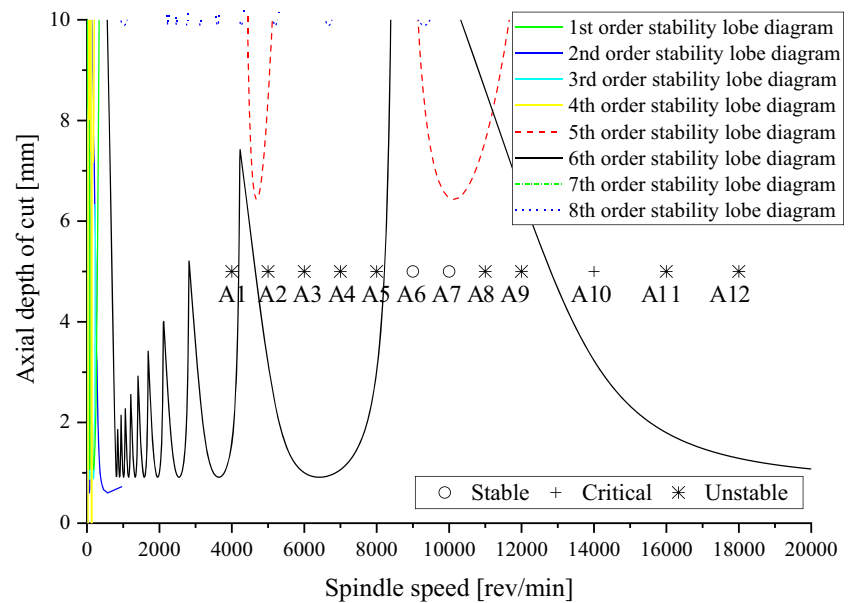
Fig. 12 Representative finished surface recorded from group (**a**) A9 and (**b**) A12
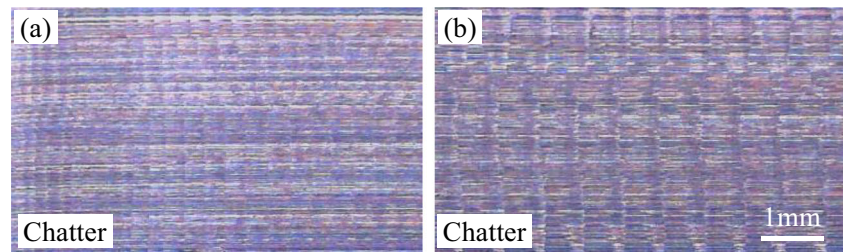
amplitude and amplitude of non-dominant frequency after 2500-Hz low pass filter suddenly and greatly decreased. The proposed method was validated by experimental works, the stability predicted with acoustic emission signals based on the RMS value and frequency domain analysis was generally consistent with calculated results from the stability lobe diagram.

Data Availability Not applicable.

Declarations

Ethics approval Not applicable.

Consent to participate Not applicable.

Consent for publication Not applicable.

Competing interests The authors declare no competing interests.

References

1. Li J, Li B, Shen N, Qian H, Guo Z (2017) Effect of the cutter path and the workpiece clamping position on the stability of the robotic milling system. Int J Adv Manuf Technol 89:2919–2933. https://doi.org/10.1007/s00170-016-9759-x

2. Devillez A, Dudzinski D (2007) Tool vibration detection with eddy current sensors in machining process and computation of stability lobes using fuzzy classifiers. Mech Syst Signal Pr 21(1):441–456. https://doi.org/10.1016/j.ymssp.2005.11.007

3. Chen Y, Dong F (2013) Robot machining: recent development and future research issues. Int J Adv Manuf Technol 66:1489–1497. https://doi.org/10.1007/s00170-012-4433-4

4. Quintana G, Ciurana J (2011) Chatter in machining processes: a review. Int J Mach Tool Manu 51(5):363–376. https://doi.org/10.1016/j.ijmachtools.2011.01.001

5. Yue C, Gao H, Liu X, Liang ST, Wang L (2019) A review of chatter vibration research in milling. Chin J Aeronaut 32(2):215–242. https://doi.org/10.1016/j.cja.2018.11.007

6. Gasparetto A (1998) A System Theory Approach to mode coupling chatter in machining. ASME J Dyn Sys Meas 120(4):545–547. https://doi.org/10.1115/1.2801501

7. Pan Z, Zhang H, Zhu Z, Wang J (2006) Chatter analysis of robotic machining process. J Mater Process Technol 173(3):301–309. https://doi.org/10.1016/j.jmatprotec.2005.11.033

8. Tunc LT, Stoddart D (2017) Tool path pattern and feed direction selection in robotic milling for increased chatter-free material removal rate. Int J Adv Manuf Technol 89:2907–2918. https://doi.org/10.1007/s00170-016-9896-2

9. Gasparetto A (2001) Eigenvalue analysis of mode-coupling chatter for machine-tool stabilization. J Vib Control 7(2):181–197. https://doi.org/10.1177/107754630100700203

10. Verl A, Valente A, Melkote S, Brecher C, Ozturk E, Tunc LT (2019) Robots in machining. CIRP Ann 68(2):799–822. https://doi.org/10.1016/j.cirp.2019.05.009

11. Cen L, Melkote SN (2017) CCT-based mode coupling chatter avoidance in robotic milling. J Manuf Process 29:50–61. https://doi.org/10.1016/j.jmapro.2017.06.010

12. Mousavi S, Gagnol V, Bouzgarrou BC, Ray P (2018) Stability optimization in robotic milling through the control of functional redundancies. Robot Cim-Int Manuf 50:181–192. https://doi.org/10.1016/j.rcim.2017.09.004

13. Cordes M, Hintze W, Altintas Y (2019) Chatter stability in robotic milling. Robot Cim-Int Manuf 55:11–18. https://doi.org/10.1016/j.rcim.2018.07.004

14. Chen C, Peng F, Yan R, Tang X, Li Y, Fan Z (2020) Rapid prediction of posture-dependent FRF of the tool tip in robotic milling. Robot Cim-Int Manuf 64:101906. https://doi.org/10.1016/j.rcim.2019.101906

15. Altintaş Y, Budak E (1995) Analytical prediction of stability lobes in milling. CIRP Ann 44(1):357–362. https://doi.org/10.1016/S0007-8506(07)62342-7

16. Insperger T, Stépán G (2002) Semi-discretization method for delayed systems. Int J Numer Methods Eng 55(5):503–518. https://doi.org/10.1002/nme.505

17. Ding Y, Zhu L, Zhang X, Ding H (2010) A full-discretization method for prediction of milling stability. Int J Mach Tool Manu 50(5):502–509. https://doi.org/10.1016/j.ijmachtools.2010.01.003

18. Hajdu D, Insperger T, Stepan G (2015) The effect of non-symmetric FRF on machining: a case study. In: Proceeding of the ASME 2015 International Design Engineering Technical Conferences and Computers and Information in Engineering Conference, August 2-5, Boston, Massachusetts, USA. https://doi.org/10.1115/DETC2015-47037

19. Tangjitsitcharoen S, Pongsathornwiwat N (2013) Development of chatter detection in milling processes. Int J Adv Manuf Technol 65:919–927. https://doi.org/10.1007/s00170-012-4228-7

20. Altintas Y, Eynian M, Onozuka H (2008) Identification of dynamic cutting force coefficients and chatter stability with process damping. CIRP Ann 57(1):371–374. https://doi.org/10.1016/j.cirp.2008.03.048

21. Yao Z, Mei D, Chen Z (2010) On-line chatter detection and identification based on wavelet and support vector machine. J Mater Process Technol 210(5):713–719. https://doi.org/10.1016/j.jmatprotec.2009.11.007

22. Delio T, Tlusty J, Smith S (1992) Use of audio signals for chatter detection and control. ASME J Eng Ind 114(2):146–157. https://doi.org/10.1115/1.2899767

23. Li X (2002) A brief review: acoustic emission method for tool wear monitoring during turning. Int J Mach Tool Manu 42(2):157–165. https://doi.org/10.1016/S0890-6955(01)00108-0

24. Matsuoka S, Shimizu K, Yamazaki N, Oki Y (1999) High-efficient end milling of an articulated robot and its characteristics. J Mater Process Technol 95(1-3):83–89. https://doi.org/10.1016/S0924-0136(99)00315-5

25. Denkena B, Bergmann B, Lepper T (2017) Design and optimization of a machining robot. Proc Manuf 14:89–96. https://doi.org/10.1016/j.promfg.2017.11.010

26. Ribeiro KSB, Venter GS, Rodrigues AR (2020) Experimental correlation between acoustic emission and stability in micromilling of different grain-sized materials. Int J Adv Manuf Technol 109:2173–2187. https://doi.org/10.1007/s00170-020-05711-1

27. Inasaki I (1998) Application of acoustic emission sensor for monitoring machining processes. Ulrasonics 36(1-5):273–281. https://doi.org/10.1016/S0041-624X(97)00052-8

28. Chiou RY, Liang ST (2000) Analysis of acoustic emission in chatter vibration with tool wear effect in turning. Int J Mach Tool Manu 40(7):927–941. https://doi.org/10.1016/S0890-6955(99)00093-0

29. Jemielniak K, Arrazola PJ (2008) Application of AE and cutting force signals in tool condition monitoring in micro-milling. CIRP J Manuf Sci Technol 1(2):97–102. https://doi.org/10.1016/j.cirpj.2008.09.007

30. Liu X, Ahmad F, Yamazaki K, Mori M (2005) Adaptive interpolation scheme for NURBS curves with the integration of machining dynamics. Int J Mach Tool Manu 45(4-5):433–444. https://doi.org/10.1016/j.ijmachtools.2004.09.009

31. Kang MC, Kim JS, Kim JH (2001) A monitoring technique using a multi-sensor in high speed machining. J Mater Process Technol 113(1-3):331–336. https://doi.org/10.1016/S0924-0136(01)00698-7

32. Feng J, Sun Z, Jiang Z, Yang L (2016) Identification of chatter in milling of Ti-6Al-4V titanium alloy thin-walled workpieces based on cutting force signals and surface topography. Int J Adv Manuf Technol 82:1909–1920. https://doi.org/10.1007/s00170-015-7509-0

33. Zhang Z, Li H, Meng G, Tu X, Cheng C (2016) Chatter detection in milling process based on the energy entropy of VMD and WPD. Int J Mach Tool Manu 108:106–112. https://doi.org/10.1016/j.ijmachtools.2016.06.002